International Journal of Pharmaceutics 682 (2025) 125918

Contents lists available at ScienceDirect

International Journal of Pharmaceutics

journal homepage: www.elsevier.com/locate/ijpharm

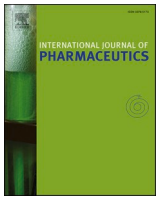

Ranking of apparent drug affinity to mesoporous silica utilizing a chromatographic screening method and a tree-based prediction model

Andreas Niederquell [a,b], Barbora Vraníková [a], Martin Kuentz [b,*]

[a] Department of Pharmaceutical Technology, Faculty of Pharmacy in Hradec Králové, Charles University, Akademika Heyrovského 1203, 500 05 Hradec Králové, Czech Republic
[b] Institute for Pharma Technology, University of Applied Sciences and Arts Northwestern Switzerland, School of Life Sciences FHNW, Hofackerstr. 30 4132 Muttenz, Switzerland

ARTICLE INFO

Keywords:
Hydrophilic interaction liquid chromatography
Apparent drug-silica interaction
Chromatographic screening
Machine learning
Classification tree model

ABSTRACT

Mesoporous silica has emerged as a promising component in bio-enabling formulation strategy. However, there is currently a lack of predictive tools for assessing drug-silica interactions in a preformulation phase, when formulators only have minimal material to guide them. This study proposes a solution: a chromatographic method to rank apparent drug-silica affinity for mesoporous formulations. Using a dataset of 52 drugs, a hydrophilic liquid interaction chromatography (HILIC) screening method was developed, with a stationary silica phase to simulate the drug carrier. Molecular descriptors were calculated for various compounds to analyze HILIC retention times using a tree-based machine learning algorithm. For silica affinity, the distribution coefficient (LogD), the molecular shape descriptor Kappa1, and the number of conjugated bonds (NCB) were identified as possible critical parameters. Additionally, an amine-modified HILIC column was evaluated to simulate a surface-modified silica carrier. The classification tree analysis revealed that Abraham's hydrogen bonding acidity, the NCB and the pKa were determinants for a qualitative assessment of drug affinity to the modified silica. The classification into low, moderate, and high affinity to the stationary phase appeared to be useful in understanding drug release from mesoporous silica formulations, highlighting its potential for future research.

1. Introduction

Modern drug discovery pipelines have an increasing occurrence of poorly water-soluble drug candidates, particularly those classified as type II according to the Biopharmaceutical Classification System (BCS) (Letzel, 2019). This trend poses significant challenges for formulation scientists, especially regarding oral formulation development and for compounds beyond the chemical space outlined by the rule of five (Lipinski et al., 2001). Modern pharmaceutical profiling and drug discovery must thus anticipate the need for bio-enabling formulations and discover which formulation technology best suits a given molecule (Kuentz et al., 2021). One promising delivery approach involves the use of mesoporous silica (McCarthy et al., 2016; Prestidge et al., 2007; Qian and Bogner, 2012; Santos et al., 2011; Suib, 2017; Vallet-Regí et al., 2018). Although mesoporous silica-based products have not yet reached the pharmaceutical market, this formulation strategy has garnered considerable global interest, with numerous research groups exploring its potential (Prestidge et al., 2007; Santos et al., 2011; Vallet-Regí et al., 2018). Moreover, as the first studies on humans and animals using mesoporous silica formulations were conducted several years ago (Bukara et al., 2016; Riikonen et al., 2013), we can soon expect to see marketed mesoporous silica formulations. Despite the substantial research interest in these formulations, there is a notable lack of practical screening and modeling approaches for early development. There are especially tools missing that predict or assess drug-silica interactions at the drug discovery stage, when only minimal drug amounts are available (Murray et al., 2023). In terms of physics-based modeling, previous work used molecular mechanics, molecular dynamics and large-scale quantum-chemical calculations to study drug interactions with silica (Delle Piane et al., 2014; Niederquell et al., 2023; Yani et al., 2016). While some calculations are fast, such as predicting critical pore size for drug nanoconfinement (Knapik et al., 2016; Mellaerts et al., 2007; Rengarajan et al., 2008; Vraníková et al., 2020) others, such as those based on quantum chemistry, require substantial computational

* Corresponding author at: Institute for Pharma Technology, University of Applied Sciences and Arts Northwestern Switzerland, School of Life Sciences FHNW, Hofackerstr. 30 4132 Muttenz, Switzerland.
E-mail address: martin.kuentz@fhnw.ch (M. Kuentz).

https://doi.org/10.1016/j.ijpharm.2025.125918
Received 14 March 2025; Received in revised form 18 June 2025; Accepted 30 June 2025
Available online 1 July 2025

resources. The latter are even more challenging when a comparatively large pore model is constructed in silico. Development of fast experimental screening methods is thus an interesting alternative research field. Data generated could then be used for a machine learning approach, but such data-driven modeling relies on a viable experimental screening protocol.

An interesting recent study used an experimental thin-layer chromatographic method with silica gel plates to estimate molecular interactions between drugs and mesoporous silica (Benedikt Brenner et al., 2024). Natural products (Coenzyme Q10, astaxanthin) and synthetic drugs (probucol, lumefantrine) were dissolved in dichloromethane and eluted with a mixture of organic solvents (petroleum ether, ethyl acetate and acetic acid). However, evaluation of this basic method only involved visual interpretation of the results. In addition, thin-layer plates have limited separation resolution, and the method had no water layer. Accordingly, there is a need to develop a high-performance chromatography-based method that uses water in the mobile phase and enables automated, reliable detection of retention time to study many compounds in a short time, in line with the needs of a discovery or preformulation stage.

An initial goal of this study was to develop an experimental chromatographic method capable of rapid and reproducible screening of drug molecules for their apparent interaction with silica surfaces. Unlike the intrinsic interactions of binary drug-silica systems, so-called apparent drug-carrier interactions take place in a liquid, which is important for both drug loading and release processes. Accordingly, a novel analytical approach is proposed for screening such an apparent drug affinity by means of hydrophilic liquid chromatography (HILIC).

HILIC was originally used to characterize interactions using biologically relevant binding agents as the stationary phase (Hage, 2006; Olsen, 2001). In the late 1970 s, combining affinity chromatography and HPLC led to the development of high-performance liquid affinity chromatography (HPAC) with more robust inorganic materials such as mesoporous silica beads and modified surfaces for pharmaceutical analyses (Rodriguez et al., 2020). The typical HILIC setup (a hydrophilic stationary phase and an aqueous polar eluent) is currently the predominant technique to separate polar drugs, which are usually otherwise poorly retained in most common reversed-phase liquid chromatography (RPLC) approaches (Alpert, 1990).

HILIC separation processes are in essence multimodal, involving drug partitioning into or out of the silica surface water layer, as well as interactions with the stationary phase. Silica surfaces can act as hydrogen bond donors and acceptors, and have different kinds of silanol groups (Vansant et al., 1995). Moreover, the deprotonation behavior of such surface silanols varies with their structural environment: isolated silanols have a pKa around 2, geminal silanols around 8, and vicinal silanols up to 13 (Rosenholm and Lindén, 2008). Hydrogen bonding, especially with isolated silanol groups, is the most common interaction mechanism with drug molecules (Gierada et al., 2019; Sjijberg, 1996). The surface charge of silica is pH-dependent, with an isoelectric point near pH 2; it becomes negatively charged above this pH and positively charged below. Studies using bare and functionalized SBA-15 mesoporous silica demonstrated that drug-silica interactions occur via hydrogen bonding or electrostatic forces, influenced by both pH and drug chemistry (Song et al., 2005). Amino-functionalized silica, by contrast, exhibits positive surface charge below pH 9 due to protonated amine groups. Thus, the medium's pH and the nature of ionizable surface groups jointly govern the silica's charge state (Rosenholm and Lindén, 2008).

In the present study, to the best of our knowledge, HILIC analytics is used for the first time to assess mesoporous silica as a possible bio-enabling formulation approach in early formulation development. HILIC columns packed with porous bare silica and amine-modified silica beads were used to simulate different carrier materials in mesoporous silica-based drug formulations. The focus was on retention times as a surrogate for interaction strengths between drug molecules and the mesoporous silica surfaces in the form of a screening method. Besides the HILIC approach, another goal was to use a machine learning algorithm to study drug-silica interactions. Therefore, classification/decision trees were constructed utilizing various molecular descriptors and the experimentally obtained retention times. The resulting decision trees should assist formulation scientists in determining "formulatability" using mesoporous silica-based formulations and possible rules of thumb based on the molecular descriptors. The introduction of these new methods from experimental HILIC screening to the machine learning approach should finally provide tools for early prediction of whether mesoporous silica may provide a viable bio-enabling formulation strategy for a given drug candidate.

2. Materials and methods

2.1. Materials

The drugs econazole, bifonazole, carbamazepine, glibenclamide, (S)-(+)-ibuprofen, loratadine, lovastatin, probucol, tenofovir, ritonavir, lopinavir, theophylline, hesperetin, baicalin, miconazole, (+)-felodipine, ivermectin, diclofenac (free acid), cinnarizine, ketoconazole, carvedilol, nimesulide, pimozide, dipyridamole and tolfenamic acid were purchased from Carbosynth Ltd. (Compton, United Kingdom). Griseofulvin, fenofibrate, indomethacin, sulfadiazine, sulfathiazole, sulfanilamide, clotrimazole, niclosamide, haloperidol, piperine, quinidine, caffeine, albendazole, benzamide, lidocaine, mebendazole, mefenamic acid, tolbutamide, flufenamic acid, uracil, naphthalene, ammonium formate, and the solvents acetone and toluene were obtained from Sigma-Aldrich LLC. (Steinheim, Germany). Indapamide was bought from AK Scientific Inc. (California, USA), celecoxib from Interchim SA (Montluçon, France), flurbiprofen from Thermo Fischer Scientific Inc. (Geel, Belgium), mesalazine from Thermo Fischer LLC. (Kandel, Germany). Progesterone was purchased from Fluka Chemical Plc. (Buchs, Switzerland), danazol from Sanofi Aventis Holdings Limited (Birmingham, United Kingdom), ketoprofen from βetaPharma & Co Ltd. (Shanghai, China) and acetylsalicylic acid from Hänseler Plc. (Herisau, Switzerland). The chemicals for the HPLC and dissolution analysis, namely acetonitrile, acetic acid, ammonium formate and the surfactant dioctyl sodium sulfosuccinate (DOSS), were obtained from Sigma-Aldrich Chemie Ltd. (Darmstadt, Germany). Acetone and dichloromethane were used for drug loading of the mesoporous silica and bought also from Sigma-Aldrich Chemie Ltd. (Darmstadt, Germany). Parteck® SLC 500 was kindly donated by Merck KGaA (Darmstadt, Germany). The water used throughout the study was prepared with an Arium® 61,215 water purification system from Sartorius Stedim Biotech Ltd. (Göttingen, Germany). All excipients were used as supplied without any further purification.

2.2. Methods

2.2.1. Sample preparation for the screening method

Saturated solutions of 52 active pharmaceutical ingredients (APIs) and 3 reference substances in pure acetonitrile were prepared as follows: after addition of excess API to 5 ml acetonitrile, the samples were stirred for 48 h on a magnetic stirring plate at 800 rpm. Afterwards, the samples were filtered using Spartan3 Syringe filter (0.45 μm PTFE) and four individual diluted samples were prepared in 2 ml HPLC vials. Based on preliminary experiments, dilution levels were set individually to reach optimal UV signal strength for each substance (Table 1).

2.2.2. HPLC-HILIC screening method

For screening measurements, an HPLC system consisting of Agilent 1200 (autosampler), 1260 (degasser and gradient pump) and 1290 (diode array detector) series components from Agilent Technologies LLC. (Waldbronn, Germany) was employed. A hydrophilic interaction liquid chromatography (HILIC) Infinitylab Poroshell 120 (4.6 x 250 cm)

Table 1
UV detection wavelengths (nm) and sample dilution levels (v/v) in pure acetonitrile of 50 APIs from the HPLC-HILIC experiments (n = 4).

Drug	Wavelength (nm)	Dilution level (v/v)	Drug	Wavelength (nm)	Dilution level (v/v)
Acetylsalicylic acid	276	1:100	Ivermectin	245	1:500
Albendazole	230	1:200	Ketoconazole	244	1:100
Benzamide	254	1:200	Ketoprofen	255	1: 500
Bifonazole	256	1:500	Lidocaine	244	1:100
Caffeine	220	1:500	Lopinavir	215	1:200
Carbamazepine	215	1:500	Loratadine	243	1:500
Carvedilol	240	1:500	Lovastatin	238	1:500
Celecoxib	247	1:500	Mebendazole	234	1:2
Cinnarizine	254	1:500	Mefenamic acid	286	1:20
Clotrimazole	233	1:500	Mesalazine	275	1:2
Danazol	285	1:200	Miconazole	233	1:500
Diclofenac	270	1:500	Niclosamide	275	1:200
Dipyridamole	276	1:20	Nimesulide	265	1:500
Econazole	230	1:500	Pimozide	280	1:100
Felodipine	234	1:500	Piperine	240	1:500
Fenofibrate	240	1:500	Probucol	242	1:500
Flufenamic acid	286	1:500	Progesterone	240	1:500
Flurbiprofen	247	1:500	Quinidine	235	1:500
Glibenclamide	230	1:200	Ritonavir	215	1:200
Griseofulvin	291	1:500	Sulfadiazine	270	1:500
Haloperidol	240	1:100	Sulfanilamide	270	1:500
Hesperetin	284	1:500	Sulfathiazole	265	1:200
Ibuprofen	214	1:500	Theophylline	272	1:200
Indapamide	235	1:500	Tolbutamide	240	1:500
Indomethacin	260	1:500	Tolfenamic acid	286	1:100

column from Agilent Technologies Plc. (Basel, Switzerland) was used as stationary phase for simulating a mesoporous silica carrier. The column packing material consisted of 4 μm superficially porous bare silica beads (surface area: 130 m^2/g and pore size:120 Á). A second HILIC column was used to represent a surface modified mesoporous silica formulation, with amino group modified surfaces (propyl bound amino groups with a surface area of 320 m^2/g and a pore volume of 0.8 ml/g according to the manufacturer; for comparison, Parteck® SLC 500 was found to have a pore volume of 0.83 cm^3/g and a surface area of 495.8 m^2/g (Vraníková et al., 2020)); The amine modified carrier model was a VDSpher Pur 100 NH_2 column that was obtained from BGB Analytik Plc. (Boeckten, Switzerland). The column had identical dimensions (4.6 x 250 cm) and silica particle size (4 μm). Individual compound dilution levels in pure acetonitrile (quadruplicates) and UV detection wavelengths were determined in pre-experimental runs (Table 1).

Further method optimization involved several pretests regarding optimal flow rates and mobile phase compositions. This resulted in the following gradient pump setup: for the first two minutes, the mobile phase consisted of 99 % acetonitrile and 1 % water with 100 mM ammonium formate. The first slower gradient changed the composition to 6 % water (100 mM ammonium formate) within 30 min. A second gradient increased water content from 6 % to 15 % within 5 min. Afterwards, the mobile phase composition was reverted to 1 % water (100 mM ammonium formate) content and 99 % acetonitrile within 3 min, and for the next 20 min, this composition was kept constant for HILIC column recovery and for the buildup of the water layer on the silica surfaces. With this setup, an average pressure of 53 bar was achieved. During all sample injections (10 μl), a constant flow rate of 800 μl/min was used. The pH of the mobile phase containing 6 % to 15 % (v/v) water with ammonium formate ranged from 6.9 to 7.2 at 25 °C. The dead volume time was determined by the retention time of the fastest eluting substances (probucol for the bare silica column and fenofibrate for the amine-modified HILIC column), and corrected retention times for this dead volume time were used for the subsequent data modeling. All measurements were done in quadruplicate at room temperature (25 °C). Retention times were obtained from the retention peaks using ChemStation for LC 3D Systems analyzing software (Rev. B.04.03-SP2 [105]).

2.2.3. Tree-based classification modeling of HILIC retention times

50 APIs and 3 reference substances (naphthalene, uracil and toluene) were empirically chosen for statistical evaluation. COSMOQuick v. 1.7 from COSMOlogic-Dassault Systems (Leverkusen Germany) was utilized as a graphic interface to retrieve 19 arbitrarily selected molecular descriptors for the used active substances from the integrated open-source chemoinformatics software package RDKit (www.rdkit.org). 13 additional molecular descriptors and physicochemical properties were gathered manually from publicly available databases such as ChemSpider and Drugbank, for example values predicted by ACD Labs (Toronto, Canada). Prior to using a tree-based machine learning algorithm with experimental data, the corrected retention times were taken as measures of drug-silica interaction strength, and instead of parametric values, categories were considered for statistical analysis. Thus, corrected retention times were first converted according to their values into three categories: fast (F) for bare silica: < 1.81 min and amine-modified silica: < 1.95 min; medium (M) for bare silica: 1.81 – 9.89 min and amine-modified silica: 1.95 – 16.50 min; and slow (S) for bare silica: > 9.89 min and amine-modified silica: > 16.50 min). The molecular descriptors (in total 32) were then used as independent variables for the classification tree analysis using Statgraphics Centurion v. 19.6.06 by Statgraphics Technologies Inc. (The Plains, USA). In this context, baicalin and tenofovir were identified as statistical outliers and were therefore not considered for the finally obtained classification trees. Statgraphics has an interface to the "R" statistical computing software (v. 4.3.3) and the calculations were based on the "tree" package in R from the R foundation for statistical computing (Vienna, Austria). The decision tree model parameters, which govern the partitioning of the tree into branches and leaves, were maintained at their default settings. Specifically, the smallest allowable node size was set to 10, and the minimum number of observations required in each child node after a split was 5. By default, the tree package stops partitioning when each branch has fewer than 5 samples. The minimum within-node deviance required for a split was 0.01. For pruning, which simplifies the trees by trimming branches, the number of leaves was limited to 5. The dataset was divided into a training set, comprising the first 41 substances, and a validation set consisting of the remaining 12 substances; tree bifurcations were constructed until a minimum residual mean deviance (RMD) was obtained. This RMD is the total residual deviance divided by the number of observations minus the number of terminal nodes, and the total residual deviance is the sum of squares of the residuals, for a classification tree, the RMD is defined by Equation (1) (Polhemus,

2018):

$$RMD = \frac{\sum_{i=1}^{n} - 2\log(p_{i,j})}{n-k} \quad (1)$$

where n is the number of substances in the training set, k is the number of subgroups or leaves in the tree and $P_{i,j}$ is the estimated probability that substance i would be assigned to category i and j is the category predicted by the model (Polhemus, 2018). Smaller RMD values correspond to better-predicting trees in the training data set. The training set was utilized to construct the decision tree, while the validation set, with 4 arbitrarily chosen substances from each retention time category (fast, medium and slow), was used to assess the model's accuracy by automated analysis of correctly and incorrectly assigned categories. In addition to the tree-based analysis, Statgraphics Centurion was used to perform an analysis of variance (ANOVA), followed by a multiple range test using Fisher's least significant difference (LSD) method to identify statistically significant differences between group means to evaluate drug release from mesoporous silica formulations.

2.2.4. Experimental comparison with selected model formulations

2.2.4.1. Drug loading of disordered mesoporous silica. Parteck® SLC 500 was loaded with probucol, lopinavir and ketoconazole using the incipient wetness impregnation method and with individually calculated theoretical monolayer capacity (MLC) concentrations for each drug according to Equation (2) (Le et al., 2019):

$$MLC = \frac{SSA\ M_w\ 10^{20}}{SA_M\ N_A}\left[\%, g_{drug}\Big/ g_{silica}\right] \quad (2)$$

where SSA is the specific surface area of the mesoporous carrier, M_w is the molecular weight of the drug, SA_M is the maximum projected contact area of a single molecule, calculated using the two largest molecular dimensions of the drug molecule, and N_A is the Avogadro's number. The molecular dimensions of the drug molecules were obtained after energy minimization using Chemica Electrica Gateway GUI software with Molecular Modeling Pro Plus 8.2.1 (Norgwyn Montgomery Software Inc., North Wales, USA). Further details on the MLC calculation and the specific surface area measured by BET for Parteck® SLC 500 are described elsewhere (Le et al., 2019; Niederquell et al., 2023; Vraníková et al., 2020).

The incipient wetness impregnation method was performed on a Chemyx Fusion 200 (Chemyx Inc., USA) syringe pump. To remove most of the water prior to the loading step, the mesoporous silica carrier was dried for 12 h at 80 °C using a KVTS 11 vacuum oven from Salvis Plc. (Reussbühl, Switzerland) at 550 mbar atmospheric pressure. Loading solvents were chosen individually according to best solubility based on pre-experiments. Acetone was used for lopinavir, and dichloromethane for probucol and ketoconazole. The drug solutions had a concentration of 20 mg/ml and were applied dropwise to 1.0 g of the stirred mesoporous silica material (magnetic stirring plate at 50 rpm) at a pumping speed of 0.1 ml/min. According to the calculated MLC, individual volumes of the drug solutions were dosed (probucol 22.6 % w/w, lopinavir 19.34 % w/w, and ketoconazole 12.4 % w/w). For the following solvent removal and drying step, the drug-loaded mesoporous silica samples were placed in the vacuum oven for 24 h at 60 °C and 500 mbar. The actual drug load was checked gravimetrically as the mass difference before and after drug loading of the dried samples, using an analytic balance XS205DU from Mettler Toledo Ltd. (Greifensee, Switzerland).

2.2.4.2. In vitro non-sink dissolution tests using three drug-loaded mesoporous silica formulations. Comparative dissolution experiments were done for selected model formulations using a USP 2 dissolution apparatus DT 600 from Erweka Ltd. (Langen, Germany). Phosphate buffer with a pH of 6.8 and 0.5 % (w/v) dioctyl sodium sulfosuccinate (DOSS) from Sigma-Aldrich Chemie Ltd. (Darmstadt, Germany) was used as the dissolution medium. Each vessel contained 250 ml dissolution medium; after adding 120 mg powdery formulation sample, 2 ml sampling volumes were taken after 2, 3, 4, 5, 10, 15, 20, 30, 40 50, 60, 75, 90, 120, 150 and 180 min. The volume was kept constant using fresh buffer at 37 ± 0.5 °C. Samples were filtered with a syringe filter with PTFE membrane (Titan HPLC-Filter 17 mm/ 0.45 µm) from Infochroma Plc. (Goldau, Switzerland). All experiments were performed in triplicate at 37 ± 0.5 °C using 25 rpm paddle speed. Dissolution curves were shown as cumulative concentrations versus sampling time.

2.2.4.3. Equilibrium solubility in release medium. Saturated drug samples (4 ml) in dissolution medium (phosphate buffer at pH 6.8) were prepared by stirring for 24 h at 200 rpm on a magnetic stirring plate at 37 °C. Afterwards, they were centrifuged at 15,000 rpm for 10 min using an Eppendorf 5420 Microcentrifuge from Eppendorf Plc. (Hamburg, Germany) and filtered using Titan HPLC-Filter (Ø 17 mm/0.45 µm) with a PTFE membrane. Prior to concentration determinations by means of HPLC, samples were diluted with dissolution buffer medium. Calibration curves were prepared using three individual saturated stock solutions in pure acetonitrile. After filtration with titan HPLC syringe filters (0.45 µm), dilutions from each stock solution were done (1:2, 1:4, 1:8, 1:16, 1:32, 1:64, and 1:100) considering the calculated MLC of each drug (the monolayer value was the highest concentration of the calibration curve). All sample measurements, stock solutions and dilutions were done in triplicate at 25 °C. Injection volume was 10 µl; a flow rate of 800 µl/min was used for ivermectin and quinidine, and 600 µl/min for lopinavir. A XBridge BEH C18 column from Waters Ltd. (Eschborn, Germany) was used (130 Å mean pore size and 5 µm particle size, inner diameter 4.6 mm and 150 mm length). Different mobile phase compositions were used for each drug: for probucol, 98 % (v/v) acetonitrile, 2 % (v/v) ultrapure water and UV wavelength 242 nm; for lopinavir, 70 % (v/v) acetonitrile, 30 % (v/v) ultrapure water at 215 nm; for ketoconazole, 70 % (v/v) acetonitrile, 30 % (v/v) ultrapure water with 0.1 % (v/v) acetic acid and 10 mM ammonium acetate at a pH of 4.5 and 244 nm.

3. Results and discussion

3.1. HILIC experiments and tree-based predicted drug categories

The utilization of mesoporous silica as a formulation carrier still poses numerous open questions regarding interactions between drug molecules and the silica surfaces. There are binary drug-silica interactions that represent an intrinsic drug to carrier affinity. This can be influenced by the presence of a solvent leading to an apparent affinity of drug to silica, which is expected to be critical for processing by incipient wetness impregnation or regarding drug release from the carrier formulation (Niederquell et al., 2023). Recent investigations by Taylor's research group at Purdue University addressed the topic of apparent drug-silica interactions, focusing on drug sorption experiments to obtain a BET-isotherm, which was then compared to release behavior (Dening et al., 2019; McCarthy et al., 2020). Other approaches used either inverse gas chromatography and molecular mechanics to learn about intrinsic drug affinity to silica (Niederquell et al., 2023), or thin-layer chromatography to assess apparent drug-silica interactions (Benedikt Brenner et al., 2024). Finally, the present study aimed to develop a HILIC-based screening method to investigate apparent drug-silica interactions and further determine molecular descriptors that correlate with these molecular interactions. Fig. 1 depicts a schematic overview of the employed HPLC-HILIC screening setup with new scope to assess possible drug-silica interactions for early formulation screening.

Drug solutions were injected via the HPLC system into the HILIC column with porous silica as the stationary material. The apparent drug-silica affinities were then assessed according to the retention times. As a result of the screening experiments, tables 2 and 3 provide the measured retention times (min) on bare silica and amino group-modified silica

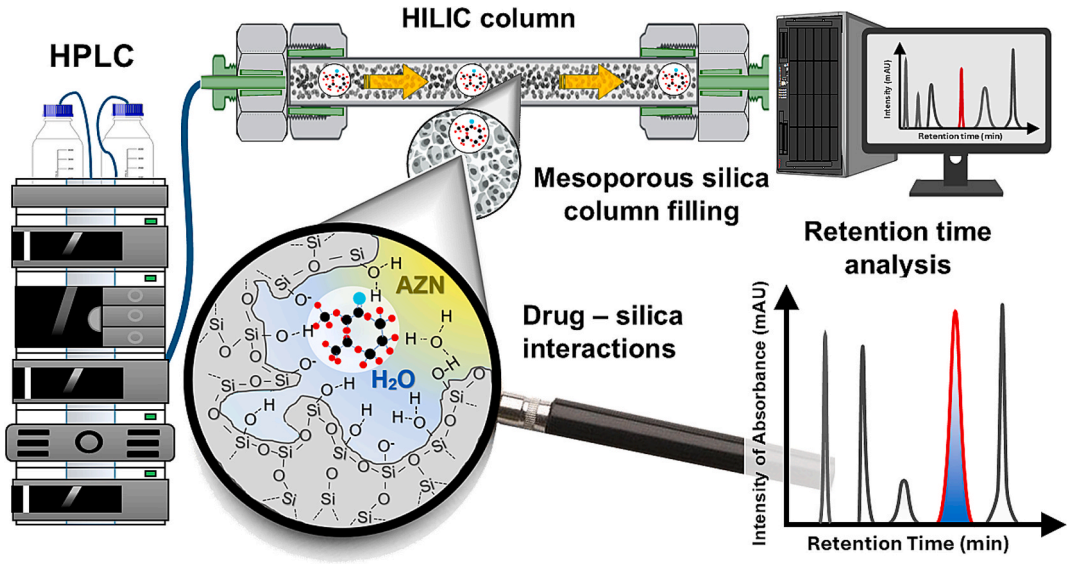

Fig. 1. Schematic overview of the HPLC-HILIC setup for screening the apparent drug-silica affinities; (AZN = Acetonitrile).

Table 2
Bare silica HILIC column – mean retention times (min) as uncorrected raw data of 50 APIs (n = 4) from the HPLC-HILIC experiments and assigned categories (F = fast, M = medium and S = slow).

Drug	Retention time (min)	Category	Drug	Retention time (min)	Category
Probucol	3.4 ± 0.1	F	Clotrimazole	6.2 ± 0.1	M
Niclosamide	3.4 ± 0.1	F	Caffeine	6.8 ± 0.0	M
Nimesulide	3.5 ± 0.1	F	Bifonazole	7.1 ± 0.0	M
Mesalazine	3.5 ± 0.1	F	Miconazole	7.3 ± 0.0	M
Celecoxib	3.6 ± 0.0	F	Econazole	7.4 ± 0.1	M
Fenofibrate	3.6 ± 0.0	F	Lidocaine	8.0 ± 0.0	M
Felodipine	3.8 ± 0.0	F	Theophylline	9.8 ± 0.1	M
Danazol	3.8 ± 0.1	F	Ritonavir	11.5 ± 0.1	M
Indapamide	3.9 ± 0.0	F	Lopinavir	12.0 ± 0.0	M
Lovastatin	4.0 ± 0.1	F	Cinnarizine	12.2 ± 0.2	M
Sulfanilamide	4.0 ± 0.0	F	Ibuprofen	13.3 ± 0.1	S
Hesperetin	4.0 ± 0.0	F	Mefenamic acid	14.3 ± 0.1	S
Progesterone	4.0 ± 0.1	F	Tolfenamic acid	16.1 ± 0.0	S
Griseofulvin	4.1 ± 0.0	F	Flufenamic acid	17.2 ± 0.1	S
Sulfadiazine	4.4 ± 0.1	F	Flurbiprofen	19.6 ± 0.2	S
Tolbutamide	4.4 ± 0.1	F	Ketoprofen	21.1 ± 0.4	S
Piperine	4.7 ± 0.1	F	Diclofenac	22.1 ± 0.1	S
Ivermectin	5.0 ± 0.0	F	Dipyridamole	23.6 ± 0.0	S
Benzamide	5.0 ± 0.0	F	Indomethacin	23.8 ± 0.2	S
Albendazole	5.1 ± 0.0	F	Ketoconazole	25.3 ± 0.0	S
Glibenclamide	5.2 ± 0.1	M	Carvedilol	27.9 ± 0.1	S
Mebendazole	5.2 ± 0.1	M	Pimozide	30.4 ± 0.0	S
Sulfathiazole	5.3 ± 0.1	M	Haloperidol	34.3 ± 0.1	S
Carbamazepine	5.5 ± 0.1	M	Acetylsalicylic acid	34.7 ± 0.0	S
Loratadine	5.8 ± 0.1	M	Quinidine	41.7 ± 0.1	S

surfaces of 50 active pharmaceutical ingredients. According to these retention times, all APIs were arbitrarily assigned to the categories fast (F), medium (M), and slow (S).

Commonly used reference substances to determine the dead volume, namely, uracil (HILIC t = 7.47 min and Amine HILIC t = 20.22 min), naphthalene (HILIC t = 3.47 min and Amine HILIC t = 3.76 min) and toluene (HILIC t = 3.55 min and Amine HILIC t = 3.73 min), were further evaluated. However, the shortest retention times were observed with probucol (3.41 min) using bare silica, and fenofibrate (3.71 min) with the amine-modified HILIC column. These values were accordingly providing better estimates of the dead volume times for the two columns, which was used to determine corrected retention times alternatively to the raw data given in Tabel 2 and 3.

When comparing both columns, it was expected to obtain an alternative ranking of compound retention times based on the different surface chemistry. Indeed, for quinidine, acetylsalicylic acid, haloperidol, pimozide, carvedilol and ketoconazole, bare silica resulted in the longest retention times (25.3 to 41.7 min). Niclosamide, mesalazine, fenofibrate, felodipine and celecoxib had the shortest retention times (< 4 min), which was not the same ranking as with the amine-modified surface (Table 3). Bare silica contains negatively charged silanol groups under moderate to basic pH conditions, enabling strong electrostatic interactions with positively charged analytes, whereas amine-containing mesoporous silica surfaces preferably retain negatively charged molecules (Bell, 2015).

Accordingly, the highest differences in retention times between the amine-modified and bare mesoporous silica surface were obtained with mesalazine (Δ = + 40.9 min), mefenamic acid (Δ = + 27.0 min) and tolfenamic acid (Δ = + 25.9 min), whereby all three compounds were expected to be negatively charged at physiological conditions (Knox

Table 3
Amine-modified HILIC column – mean retention times (min) as uncorrected raw data of 50 APIs (n = 4) from the HPLC-amine HILIC experiments and assigned categories (F = fast, M = medium and S = slow).

Drug	Retention time (min)	Category	Drug	Retention time (min)	Category
Fenofibrate	3.7 ± 0.0	F	Ivermectin	13.0 ± 0.2	M
Probucol	3.8 ± 0.3	F	Sulfadiazine	13.5 ± 0.3	M
Griseofulvin	4.2 ± 0.0	F	Ritonavir	13.9 ± 0.3	M
Progesterone	4.2 ± 0.2	F	Lopinavir	14.6 ± 0.1	M
Felodipine	4.5 ± 0.1	F	Theophylline	14.8 ± 0.6	M
Lidocaine	4.5 ± 0.0	F	Pimozide	16.6 ± 0.3	M
Cinnarizine	4.6 ± 0.2	F	Hesperetin	17.2 ± 0.4	M
Danazol	4.8 ± 0.2	F	Carvedilol	17.9 ± 0.7	M
Lovastatin	4.9 ± 0.0	F	Niclosamide	18.3 ± 0.2	M
Piperine	4.9 ± 0.2	F	Sulfathiazole	22.4 ± 0.1	S
Celecoxib	5.0 ± 0.3	F	Dipyridamole	22.4 ± 0.1	S
Loratadine	5.1 ± 0.2	F	Mebendazole	23.9 ± 0.0	S
Caffeine	5.2 ± 0.3	F	Quinidine	24.6 ± 0.3	S
Econazole	5.6 ± 0.0	F	Tolbutamide	24.8 ± 0.0	S
Bifonazole	5.7 ± 0.0	M	Glibenclamide	28.7 ± 0.1	S
Clotrimazole	5.7 ± 0.3	M	Ibuprofen	37.9 ± 0.4	S
Miconazole	5.9 ± 0.5	M	Mefenamic acid	41.6 ± 0.0	S
Benzamide	6.4 ± 0.0	M	Tolfenamic acid	42.3 ± 0.0	S
Sulfanilamide	6.6 ± 0.1	M	Flufenamic acid	42.4 ± 0.0	S
Carbamazepine	6.9 ± 0.0	M	Flurbiprofen	43.3 ± 0.6	S
Nimesulide	7.1 ± 0.2	M	Diclofenac	43.5 ± 0.0	S
Indapamide	7.5 ± 0.0	M	Ketoprofen	43.9 ± 0.2	S
Albendazole	9.5 ± 0.0	M	Indomethacin	44.5 ± 0.6	S
Ketoconazole	10.7 ± 0.1	M	Acetylsaicylic acid	44.5 ± 0.2	S
Haloperidol	12.7 ± 0.2	M	Mesalazine	44.6 ± 0.0	S

et al., 2024). On the other hand, haloperidol (Δ = – 21.9 min), quinidine (Δ = – 17.4 min) and ketoconazole (Δ = – 14.9 min) showed faster retention time on the amine-modified HILIC column. Here, ketoconazole was uncharged but the other two substances had a positive physiological charge and were most probably repelled by the same surface charge of the amino groups. However, coulombic interactions (electrostatic attraction/repulsion) are only part of the net drug surface interaction. There is also hydrogen bonding to the stationary phase or to the tightly bound water on the stationary phase (Hemström and Irgum, 2006). This emphasizes the relevance in preformulation of novel experimental screening tools such as HILIC regarding carriers based on silica and modified silica for drug delivery. Mesoporous silica surface chemistry can also be tailored to enhance or suppress the molecular interaction mechanisms, thus influencing retention and selectivity (Bell, 2015).

Fig. 2 displays a simplified schematic overview of possible interaction mechanisms between an analyte molecule and the silica surface of a HILIC column, with the example of an amine-modified surface (Fig. 2A) and a bare silica surface (Fig. 2B).

The main mechanisms of retention in HILIC have been discussed previously, which can be inferred from several review articles (Ares and Bernal, 2012; Dejaegher and Vander Heyden, 2010; Hemström and Irgum, 2006).

Based on results obtained from the HPLC-HILIC screening method, another aim of the present study was to evaluate a tree-based machine learning algorithm to link molecular descriptors with the apparent affinity to the different adsorbing surfaces. Thus, retention time was used as the dependent variable and a set of 32 drug descriptors/properties was employed in supervised classification tree analyses. Table 4 displays

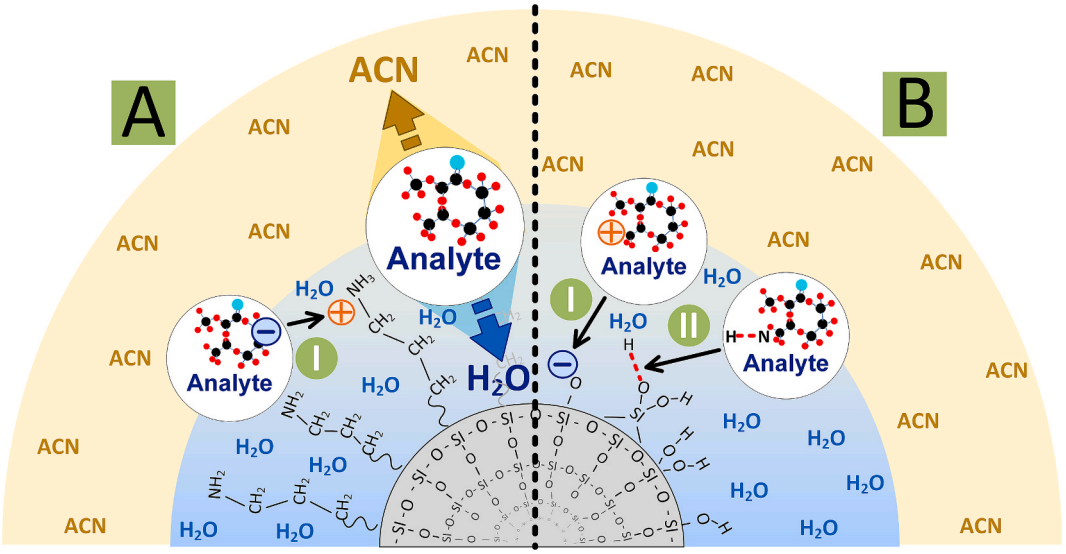

Fig. 2. Simplified scheme of hilic interaction mechanisms. (a) represents the aminopropyl-modified silica surface and (b) the bare silica surface. after hydrophilic partitioning of the analyte (center left) between the organic mobile phase (here acetonitrile = ACN) and the water-enriched layer, electrostatic interactions of ionizable compounds (process I), Van der Waals forces or hydrogen bonding (process II), and dipole–dipole interactions can occur.

Table 4
Description of the molecular descriptors identified in the final decision trees for the bare silica and amino-modified silica surface.

Relevant molecular descriptors for bare silica surface	
Log D (pH 7.5)	The logarithm of the (octanol/buffer) distribution coefficient at pH 7.5, obtained from the chemspider.com database (Pence and Williams, 2010) as calculated by the PhysChem Suite, v2024, Advanced Chemistry Development, Inc. (ACD/Labs), Toronto, ON, Canada, www.acdlabs.com
KAPPA 1	A topological descriptor representing the first-order Kier molecular shape index (Hall and Kier, 1991), which provides insights into the size, shape, and degree of branching of a molecule. This parameter was calculated using the RDKit cheminformatics software package (https://www.rdkit.org)
Conjugated bonds	The number of conjugated bonds (NCB) in a molecule, defined as alternating single and double bonds or lone pairs that allow π-electron delocalization across adjacent atoms. This descriptor reflects the extent of π-conjugation and was derived using RDKit (https://www.rdkit.org)
Relevant molecular descriptors of the amino-modified silica surface	
A	Abraham's solvation parameter for hydrogen bonding acidity
Conjugated bonds	Number of conjugated π-electron bonds obtained from the RDKit cheminformatics software (https://www.rdkit.org)
pKa strongest acidic	The solvent-dependent "acid dissociation constant" obtained from the database go.drugbank.com. (Knox et al., 2024)

the molecular properties identified by the algorithm as relevant for retention times, while Figs. 3 and 5 depict the resulting decision trees.

For this drug classification, one has to begin at the top of the tree and move left if the binary parameter statement is true, or to the right if it is false. The leaves at the terminating nodes display the predicted categories of the dependent variable.

There were 4 terminating leaves obtained for the bare silica HILIC column (Fig. 3). At the first node, compounds are separated based on LogD (pH 7.4) with a threshold of 3.5. Drugs with LogD < 3.5 are more polar and hydrophilic and tend to show stronger interactions with the polar silanol groups on the silica surface. However, bare silica surfaces contain acidic surface silanol groups meaning that under physiological conditions, these groups will be mostly deprotonated/ionized in intestinal medium (Hate et al., 2020; Rosenholm and Lindén, 2008) and depending on the charge of the molecule at pH 7.4 (acids = deprotonated, bases = protonated) electrostatic attraction or repulsion can be expected. Within this group, compounds were further differentiated by the proposed tree by Kappa1, a descriptor of molecular shape and branching. A Kappa1 value < 11.5 typically denotes smaller, less complex molecules, which were in this study classified as fast-eluting, likely due to fewer interaction points or less steric hindrance at the surface. In contrast, more complex polar drugs (Kappa1 ≥ 11.5) exhibit slower elution, consistent with increased interaction potential or decreased mobility. Compounds with LogD ≥ 3.5, indicating more hydrophobic character, generally exhibited a weaker affinity to the hydrophilic silica mostly due to a reduced capacity for hydrogen bonding. Their retention was apparently influenced by the extent of conjugation in the molecule. According to the classification tree, a low number of conjugated bonds (< 16.5) was associated with faster elution, reflecting less polarizability and limited π-surface interactions. In contrast, drugs with high conjugation (≥ 16.5) were categorized as medium retention. The extent of π-conjugation can promote Van der Waals and dispersion interactions, contributing to a moderate affinity (Radhakrishnan et al., 2023; Ringwald and Pemberton, 2000). Overall, the tree emphasizes the role of molecular polarity, structural complexity, and the extent of π-conjugation in determining drug–silica interactions. The statistical reliability of the tree analysis was represented by the error remaining in the tree after construction (i.e. RMD), which can be considered as a goodness-of-fit statistic (Ritschard, 2006). The magnitude of value deviance associated with the tree containing various numbers of leaves was also analyzed; there was only a continuous improvement until 4 leaves with 4 terminating knots were given. In the first classification tree of the bare silica column, the calculated RMD was 0.89. A further important parameter to evaluate model accuracy is the misclassification rate (MR = proportion of observations in the training set predicted to fall in another category than they did). The classification tree above had an MR of 0.24. This means that 24 % of all substances were classified incorrectly.

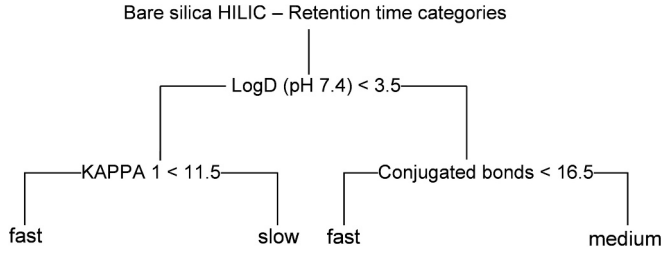

Fig. 3. Classification tree using bare silica HILIC column.

The training set consisted of 41 substances: 18 were categorized as fast, 12 as medium and 11 as slow. In total, 73.2 % of all training cases were classified correctly. For the validation set (n = 12) 4 substances belonged to each classification category. In total, 41.7 % of all validation cases were correctly classified. The following mosaic plot (Fig. 4) depicts the classifications in % for each dependent variable coded in grey shades. Here the results are shown for the combined sample set (n = 53), with each row representing a level for the dependent variable. The correct prediction for the category "fast" was made for 14 substances (64 %), whereas 0 substances (0 %) were categorized as medium and 8 (36 %) as slow. For the category "medium", 8 substances or 50 % were correctly classified, while 6 substances were assigned as fast (37 %) and 2 (13 %) as slow. 13 out of 15 slow-eluting substances (long retention time) were classified correctly (87 %) and only one substance each was incorrectly classified as fast (7 %) and medium (7 %). Accordingly, there was a higher misclassification with the categories fast and medium compared to the slow eluting substances.

In this study a second HILIC column with propyl-bound amino groups to act as a model of a surface-modified silica carrier was chosen. The silica surface modification was interesting to study for apparent drug interactions, as these could ultimately influence the drug loading

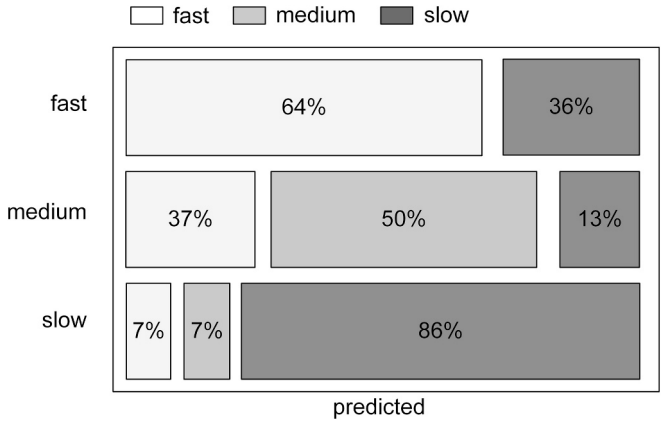

Fig. 4. Observed versus predicted mosaic plot for the bare silica HILIC column experiments (combined dataset, n = 53).

(adsorption capacities) and release process. Such surface-modified silica has been used for controlled or site-specific drug release of weakly acidic drugs (Lee et al., 2008; Song et al., 2005; Vallet-Regí et al., 2007). Another example of how surface modification can lead to altered drug loading and release properties is the study by (Martín et al., 2018), which synthesized and evaluated ten structurally and texturally distinct mesoporous silica materials. The study found that amino-functionalized materials exhibited significantly higher drug adsorption capacities and more controlled drug release profiles, characterized by notably lower release rates compared to their non-functionalized counterparts in the case of the model compound methylprednisolone sodium succinate (Martín et al., 2018). Due to these interesting changes in properties, compared to the non-modified silica surface, the second amine-modified HILIC column was chosen within this study. As a result, Fig. 5 shows the classification tree for the retention time categories using the HILIC column with an amine-modified silica surface.

The decision tree (Fig. 5) displays 4 terminating leaves; the first split of the tree is done by the Abraham's solvation parameter for acidity "A" (Niederquell and Kuentz, 2018). It defines the tendency of a molecule to act as a hydrogen bond donor or acid (strength and number of H-bonds) when surrounded by solvent molecules (hydrogen bonding acceptors) (Whaley et al., 2013). Further description of Abraham's solvation parameters can be found in the literature (Abraham et al., 2004; Jeschke et al., 2012; Vitha and Carr, 2006). The molecular descriptor "conjugated bonds" formed, the second node, while a third node was given by "pKa strongest acidic". At physiological pH in the intestine, the amine groups on the silica surface will tend to protonate and become positively charged. Similarly, moderately to strong acids (pKa $<$ 7.5) will be oppositely charged due to deprotonation and the tree reasonably suggests a slow elution time based on the expected ionic interactions with the surface. Interestingly, recent work pointed out the significance of electrostatic drug-surface interactions on the performance of mesoporous silica formulations, which appears to be generally the case (Hate et al., 2020). For the amine-modified column, fast elution was obtained with less acidic molecules and having a low number of conjugated bonds (NCB). This result can be also interpreted based on electrostatic interactions, as the positively charged surface amine groups can interact with drugs via cation-π interactions (e.g. a π-electron cloud of aromatic groups). Accordingly, the tree suggests that only with both low acidity and a low NCB was fast elution from the column obtained, in line with the expected lower molecular surface interaction strength of the drug.

The training set for the retention time classification of the amine-modified HILIC column again contained 41 substances, of which 12 were classified as fast-eluting, 16 as medium, and 13 as slow; 12 compounds were used in the validation set (4 of each classification). Overall, 68.3 % of the compounds in the training dataset were correctly classified, and the validation dataset yielded a correct classification rate of 91.7 %. The misclassification rate for the amine-modified decision tree was 21 % and for the RMD a value of 1.21 was obtained. The following amounts and percentages are the sample counts of the correctly classified substances in percent of the combined dataset. Of all 16 fast eluting compounds, 10 (63 %) were correctly predicted as fast, 6 (37 %) as medium and 0 (0.0 %) as slow. In the medium class, no substance was classified as fast, 18 substances (90 %) were successfully predicted as medium-eluting and 2 (10 %) were assigned as slow. In the slow category, 11 out of 17 (65 %) substances were accurately assigned as slow. 4 (24 %) were predicted as medium and 2 (11 %) as fast. Fig. 6 visually illustrates the described observed versus predicted classifications in percent for the combined data set (n = 53) coded as grey shades; each line depicts a level for the dependent variable.

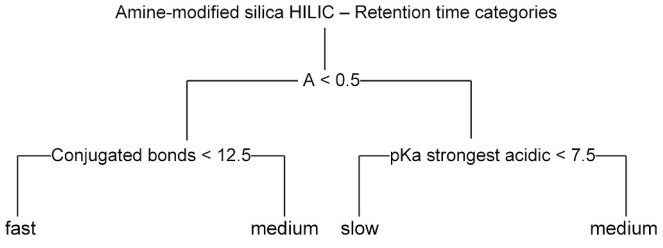

Fig. 5. Classification tree using an amine-modified silica HILIC column.

3.2. *Manufacturing and drug release of selected mesoporous silica formulations*

The aim of the present drug-carrier interaction study was to provide a characterization and screening tool for late-stage drug discovery and preformulation. Actual manufacturing and performance testing of many formulations was therefore beyond the scope of the present pilot study. However, to put the HILIC characterization into a practical perspective, one compound per category was selected as a model to compare actual drug release with what was expected based on the presented early-stage characterization.

Thus, the commonly used carrier Parteck® SLC 500 was loaded via the incipient wetness impregnation method with the lipid-lowering compound probucol, the anti-viral drug lopinavir and the antifungal active agent ketoconazole. The compounds were selected to represent each retention time classification category while targeting a similar magnitude of drug supersaturation in the release medium. The drug loadings were individually calculated according to their estimated monolayer capacity (MLC, see Table 5). Non-sink dissolution testing was performed in triplicate using 120 mg of the drug-loaded mesoporous silica formulation per vessel, under standardized conditions (37 ± 0.5 °C) for 3 h. The corresponding area under the curve (AUC) values were calculated from the resulting dissolution profiles. Solubility measurements were also conducted in triplicate, and the derived supersaturation data are presented in Table 5.

Fig. 7 presents the corresponding dissolution profiles of the three investigated drugs. The retention times from the HPLC-HILC screening experiment, and the classifications (Fast (F), Medium (M) and Slow (S)) with the molecule structures, are provided as well. In accordance with the retention time results, the concentration values show that probucol had a fast release from the mesoporous silica carrier followed by medium release kinetics of lopinavir and a comparatively slow release profile for ketoconazole. Although drugs with fast and medium HILIC retention time categorization were, with the here used model formulations, less discriminating, all drugs were correctly classified according to the trend of the mean AUC values (see Table 5). An analysis of variance (ANOVA) revealed a statistically significant difference in mean AUC

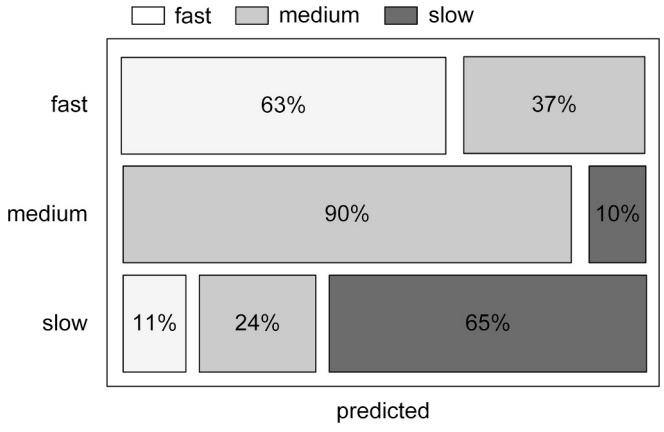

Fig. 6. Observed versus predicted mosaic plot for the amine-modified HILIC column experiments (combined dataset, n = 53).

Table 5
Overview of the area under the curve values and the supersaturation ratio at the end of the non-sink dissolution experiment (n = 3), solubility in the dissolution media, and calculated monolayer capacity for drug loading for the three used drugs in mesoporous silica formulations.

Drug	AUC of concentrations (0–180 min) [(µg·min)·mL^{-1}]	Supersaturation ratio (at 180 min) [-]	Solubility [µg/ml]	MLC [% g/g]
Probucol	6195 ± 134	0.23 ± 0.00	166.7 ± 0.02	22.6
Lopinavir	6154 ± 514	1.09 ± 0.03	34.4 ± 0.03	19.3
Ketoconazole	4741 ± 35	0.13 ± 0.00	241.9 ± 0.02	12.4

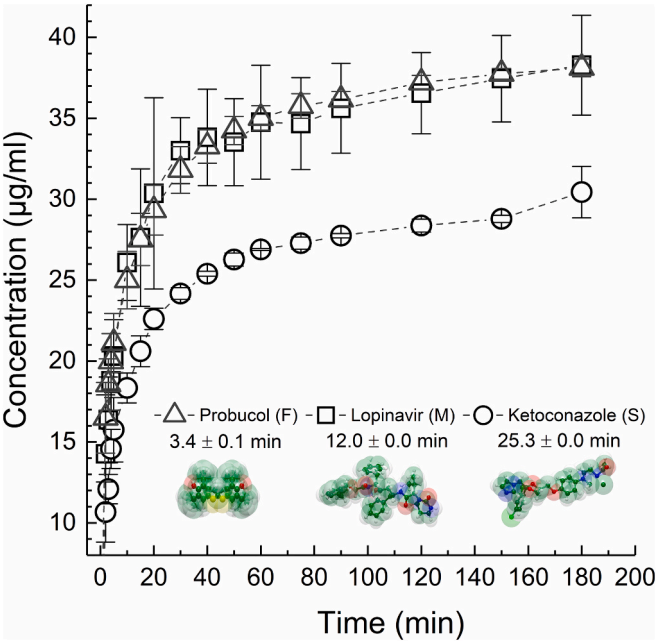

Fig. 7. Experimental *in vitro* non-sink dissolution curves (n = 3) over 3 h of probucol (triangles, fast category F), lopinavir (squares, medium category M), and ketoconazole (circles, slow category S) with mean retention times from the HPLC-HILIC screening.

values among the tested substances at the 5 % significance level (F = 13.65; p = 0.0094). A subsequent multiple range analysis using Fisher's Least Significant Difference (LSD) test revealed statistically significant differences between ketoconazole and lopinavir, as well as between ketoconazole and probucol, whereas no significant difference was found between lopinavir and probucol. These results support the hypothesis that interaction categories obtained from the novel HILIC method are indeed relevant for mesoporous formulation performance, at least regarding drug release. The drug loading of the formulations targeted the estimated monolayer capacity for standardization, also because drug release from higher drug loads (> MLC) would theoretically be affected by some drug desorption from another drug layer, which is practically independent of the carrier surface.

Even though the HILIC approach uses organic solvents such as acetonitrile, there is a significant amount of an immobilized water layer on the silica surface and at the pores. This water-rich phase is therefore deemed crucial for compound retention (Guo et al., 2019). Assuming that short retention time in the HPLC-HILIC experiment corresponds to comparatively weaker drug-silica interaction and consequently quicker release from the silica surface during dissolution (and vice versa), then the release profiles of at least the model compounds were in good agreement with the categories from the HILIC experiments. This is an encouraging result, but more research with additional manufactured formulations and their characterization would be needed to further confirm the practical relevance of the presented HILIC approach for mesoporous drug delivery.

4. Conclusions

Despite increasing interest in mesoporous silica formulations, predictive tools for assessing drug–silica interactions relevant to loading and release remain limited. Hydrophilic interaction chromatography (HILIC), a complex technique involving partitioning, polar, and ion-exchange mechanisms, was implemented as a rapid screening method using an HPLC-HILIC setup. This enabled the classification of drug substances into fast, medium, and slow eluting groups based on their apparent silica affinity. The setup is readily transferable to other academic and industrial laboratories, supporting early-stage characterization for silica-based formulation development. Retention times, combined with molecular descriptors in a machine learning framework (classification trees), yielded interpretable models to anticipate drug–silica interactions from molecular properties. However, overly simplified interpretations should be avoided: strong drug–silica interactions may impair release or promote pH-dependent re-adsorption, while weak interactions may hinder loading efficiency or lead to rapid precipitation of fast-crystallizing drugs. As such, the presented tools serve to guide a more balanced approach to formulation design. Performance assessment of drug-loaded mesoporous silica formulations based on drug-silica interaction strengths remains complex and depends on the interplay between many factors. However, the chemistry of the silica surface and that of the drug molecules are certainly key. The findings presented here offer mechanistic insight and practical guidance for future development of mesoporous silica-based drug delivery systems. Further investigations using broader drug sets, higher loads exceeding monolayer capacity, and varied pH conditions will be essential to refine and validate these tools for formulation optimization.

CRediT authorship contribution statement

Andreas Niederquell: Writing – original draft, Visualization, Methodology, Investigation, Formal analysis, Data curation, Conceptualization. **Barbora Vraníková:** Writing – review & editing, Supervision, Resources, Conceptualization. **Martin Kuentz:** Writing – review & editing, Supervision, Resources, Conceptualization.

Declaration of competing interest

The authors declare that they have no known competing financial interests or personal relationships that could have appeared to influence the work reported in this paper.

Acknowledgements

This study was supported by the Charles University (SVV 260 661), Charles University Grant Agency (Grant No. 337622/2022) and the project New Technologies for Translational Research in Pharmaceutical Sciences/NETPHARM, ID CZ.02.01.01/00/22_008/0004607, co-funded by the European Union. We thank Dr. Stefanie Feiler for her support and guidance in the statistical data evaluation. Moreover, English proof reading by Andrew Brown is gratefully acknowledged.

Data availability

Data will be made available on request.

References

Abraham, M.H., Ibrahim, A., Zissimos, A.M., 2004. Determination of sets of solute descriptors from chromatographic measurements. J. Chromatogr. A. https://doi.org/10.1016/j.chroma.2003.12.004.

Alpert, A.J., 1990. HYDROPHILIC-INTERACTION CHROMATOGRAPHY FOR THE SEPARA-TION OF PEPTIDES, NUCLEIC ACIDS AND OTHER POLAR COMPOUNDS, Journnl qf Chromatogruphy.

Ares, A.M., Bernal, J., 2012. Hydrophilic interaction chromatography in drug analysis. Cent. Eur. J. Chem. https://doi.org/10.2478/s11532-012-0003-8.

Bell, D.S., 2015. Retention and Selectivity of Stationary Phases used in HILIC. LCGC N. Am. 33, 90–101.

Benedikt Brenner, M., Wüst, M., Kuentz, M., Wagner, K.G., 2024. High loading of lipophilic compounds in mesoporous silica for improved solubility and dissolution performance. Int. J. Pharm. 654. https://doi.org/10.1016/j.ijpharm.2024.123946.

Bukara, K., Schueller, L., Rosier, J., Daems, T., Verheyden, L., Eelen, S., Martens, J.A., Van den Mooter, G., Bugarski, B., Kiekens, F., 2016. In Vivo Performance of Fenofibrate Formulated with Ordered Mesoporous Silica Versus 2-Marketed Formulations: a Comparative Bioavailability Study in Beagle dogs. J. Pharm. Sci. 105, 2381–2385. https://doi.org/10.1016/j.xphs.2016.05.019.

Dejaegher, B., Vander Heyden, Y., 2010. HILIC methods in pharmaceutical analysis. J. Sep. Sci. https://doi.org/10.1002/jssc.200900742.

Delle Piane, M., Corno, M., Pedone, A., Dovesi, R., Ugliengo, P., 2014. Large-scale B3LYP simulations of ibuprofen adsorbed in MCM-41 mesoporous silica as drug delivery system. J. Phys. Chem. C 118, 26737–26749. https://doi.org/10.1021/jp507364h.

Dening, T.J., Zemlyanov, D., Taylor, L.S., 2019. Application of an adsorption isotherm to explain incomplete drug release from ordered mesoporous silica materials under supersaturating conditions. J. Control. Release 307, 186–199. https://doi.org/10.1016/j.jconrel.2019.06.028.

Gierada, M., De Proft, F., Sulpizi, M., Tielens, F., 2019. Understanding the Acidic Properties of the Amorphous Hydroxylated Silica Surface. J. Phys. Chem. C 123, 17343–17352. https://doi.org/10.1021/acs.jpcc.9b04137.

Guo, Y., Bhalodia, N., Fattal, B., Serris, I., 2019. Evaluating the adsorbed water layer on polar stationary phases for hydrophilic interaction chromatography (HILIC). Separations 6. https://doi.org/10.3390/separations6020019.

Hage, D.S., 2006. Handbook of Affinity Chromatography, 2nd ed. Taylor & Francis Group, LLC, Lincoln, Nebraska.

Hall, L.H., Kier, L.B., 1991. The Molecular Connectivity Chi Indexes and Kappa Shape Indexes in Structure-Property Modeling. pp. 367–422. Doi: 10.1002/9780470125793.ch9.

Hate, S.S., Reutzel-Edens, S.M., Taylor, L.S., 2020. Influence of Drug-Silica Electrostatic Interactions on Drug Release from Mesoporous Silica-based Oral delivery Systems. Mol. Pharm. 17, 3435–3446. https://doi.org/10.1021/acs.molpharmaceut.0c00488.

Hemström, P., Irgum, K., 2006. Hydrophilic interaction chromatography. J. Sep. Sci. https://doi.org/10.1002/jssc.200600199.

Jeschke, P., Krämer, W., Schirmer, U., Witschel, M., 2012. Modern Methods in Crop Protection Research. Wiley-VCH Verlag & Co, KGaA, Weinheim.

Knapik, J., Wojnarowska, Z., Grzybowska, K., Jurkiewicz, K., Stankiewicz, A., Paluch, M., 2016. Stabilization of the Amorphous Ezetimibe Drug by Confining its Dimension. Mol. Pharm. 13, 1308–1316. https://doi.org/10.1021/acs.molpharmaceut.5b00903.

Knox, C., Wilson, M., Klinger, C.M., Franklin, M., Oler, E., Wilson, A., Pon, A., Cox, J., Chin, N.E.L., Strawbridge, S.A., Garcia-Patino, M., Kruger, R., Sivakumaran, A., Sanford, S., Doshi, R., Khetarpal, N., Fatokun, O., Doucet, D., Zubkowski, A., Rayat, D.Y., Jackson, H., Harford, K., Anjum, A., Zakir, M., Wang, F., Tian, S., Lee, B., Liigand, J., Peters, H., Wang, R.Q.R., Nguyen, T., So, D., Sharp, M., da Silva, R., Gabriel, C., Scantlebury, J., Jasinski, M., Ackerman, D., Jewison, T., Sajed, T., Gautam, V., Wishart, D.S., 2024. DrugBank 6.0: the DrugBank Knowledgebase for 2024 [WWW Document]. Nucleic Acids Res. Doi: 10.1093/nar/gkad976.

Kuentz, M., Holm, R., Kronseder, C., Saal, C., Griffin, B.T., 2021. Rational selection of Bio-Enabling Oral Drug Formulations – a PEARRL Commentary. J. Pharm. Sci. https://doi.org/10.1016/j.xphs.2021.02.004.

Le, T.T., Elyafi, A.K.E., Mohammed, A.R., Al-Khattawi, A., 2019. Delivery of poorly soluble drugs via mesoporous silica: Impact of drug overloading on release and thermal profiles. Pharmaceutics 11. https://doi.org/10.3390/pharmaceutics11060269.

Lee, C.H., Lo, L.W., Mou, C.Y., Yang, C.S., 2008. Synthesis and characterization of positive-charge functionalized mesoporous silica nanoparticles for oral drug delivery of an anti-inflammatory drug. Adv. Funct. Mater. 18, 3283–3292. https://doi.org/10.1002/adfm.200800521.

Letzel, T., 2019. Specifications of Gradients in Hydrophilic Interaction Liquid Chromatography (HILIC), in: Gradient HPLC for Practitioners. Wiley, pp. 175–182. Doi: 10.1002/9783527812745.ch6.

Lipinski, C.A., Lombardo, F., Dominy, B.W., Feeney, P.J., 2001. Experimental and computational approaches to estimate solubility and permeability in drug discovery and development q settings. Adv. Drug Deliv. Rev.

Martín, A., Morales, V., Ortiz-Bustos, J., Pérez-Garnes, M., Bautista, L.F., García-Muñoz, R.A., Sanz, R., 2018. Modelling the adsorption and controlled release of drugs from the pure and amino surface-functionalized mesoporous silica hosts. Microporous Mesoporous Mater. 262, 23–34. https://doi.org/10.1016/j.micromeso.2017.11.009.

McCarthy, C.A., Ahern, R.J., Dontireddy, R., Ryan, K.B., Crean, A.M., 2016. Mesoporous silica formulation strategies for drug dissolution enhancement: a review. Expert Opin. Drug Deliv. 13, 93–108. https://doi.org/10.1517/17425247.2016.1100165.

McCarthy, C.A., Zemlyanov, D.Y., Crean, A.M., Taylor, L.S., 2020. Comparison of drug release and adsorption under supersaturating conditions for ordered mesoporous silica with indomethacin or indomethacin Methyl Ester. Mol. Pharm. 17, 3062–3074. https://doi.org/10.1021/acs.molpharmaceut.0c00489.

Mellaerts, R., Aerts, C.A., Humbeeck, J.V., Augustijns, P., Van Den Mooter, G., Martens, J.A., 2007. Enhanced release of itraconazole from ordered mesoporous SBA-15 silica materials. Chem. Commun. 1375–1377. https://doi.org/10.1039/b616746b.

Murray, J.D., Lange, J.J., Bennett-Lenane, H., Holm, R., Kuentz, M., O'Dwyer, P.J., Griffin, B.T., 2023. Advancing algorithmic drug product development: Recommendations for machine learning approaches in drug formulation. Eur. J. Pharm. Sci. 191. https://doi.org/10.1016/j.ejps.2023.106562.

Niederquell, A., Kuentz, M., 2018. Biorelevant drug solubility enhancement modeled by a linear solvation energy relationship. J. Pharm. Sci. 107. https://doi.org/10.1016/j.xphs.2017.08.017.

Niederquell, A., Vraníková, B., Kuentz, M., 2023. Study of disordered mesoporous silica regarding intrinsic compound Affinity to the Carrier and Drug-Accessible Surface Area. Mol. Pharm. 20, 6301–6310. https://doi.org/10.1021/acs.molpharmaceut.3c00690.

Olsen, B.A., 2001. Hydrophilic interaction chromatography using amino and silica columns for the determination of polar pharmaceuticals and impurities. J. Chromatogr. A.

Pence, H.E., Williams, A., 2010. Chemspider: an online chemical information resource. J. Chem. Educ. https://doi.org/10.1021/ed100697w.

Polhemus Neil W., 2018. Classification and Regression Trees [WWW Document]. URL https://www.statgraphics.com/blog/classificationregressiontrees (accessed 7.25.24).

Prestidge, C.A., Barnes, T.J., Lau, C.H., Barnett, C., Loni, A., Canham, L., 2007. Mesoporous silicon: a platform for the delivery of therapeutics. Expert Opin. Drug Deliv. https://doi.org/10.1517/17425247.4.2.101.

Qian, K.K., Bogner, R.H., 2012. Application of mesoporous silicon dioxide and silicate in oral amorphous drug delivery systems. J. Pharm. Sci. https://doi.org/10.1002/jps.22779.

Radhakrishnan, S., Lejaegere, C., Duerinckx, K., Lo, W.S., Morais, A.F., Dom, D., Chandran, C.V., Hermans, I., Martens, J.A., Breynaert, E., 2023. Hydrogen bonding to oxygen in siloxane bonds drives liquid phase adsorption of primary alcohols in high-silica zeolites. Mater. Horiz. 10, 3702–3711. https://doi.org/10.1039/d3mh00888f.

Rengarajan, G.T., Enke, D., Steinhart, M., Beiner, M., 2008. Stabilization of the amorphous state of pharmaceuticals in nanopores. J. Mater. Chem. 18, 2537–2539. https://doi.org/10.1039/b804266g.

Riikonen, J., Xu, W., Lehto, V.P., 2013. Mesoporous systems for poorly soluble drugs. Int. J. Pharm. https://doi.org/10.1016/j.ijpharm.2012.09.008.

Ringwald, S.C., Pemberton, J.E., 2000. Adsorption interactions of aromatics and heteroaromatics with hydrated and dehydrated silica surfaces by Raman and FTIR spectroscopies. Environ. Sci. Technol. 34, 259–265. https://doi.org/10.1021/es980970a.

Ritschard, G., 2006. Computing and using the deviance with classification trees. 2006 Physica-Verlag Heidelberg. Doi: Doi: 10.1007/978-3-7908-1709-6_5.

Rodriguez, E.L., Poddar, S., Iftekhar, S., Suh, K., Woolfork, A.G., Ovbude, S., Pekarek, A., Walters, M., Lott, S., Hage, D.S., 2020. Affinity chromatography: a review of trends and developments over the past 50 years. J. Chromatogr. B Analyt. Technol. Biomed. Life Sci. https://doi.org/10.1016/j.jchromb.2020.122332.

Rosenholm, J.M., Lindén, M., 2008. Towards establishing structure-activity relationships for mesoporous silica in drug delivery applications. J. Control. Release 128, 157–164. https://doi.org/10.1016/j.jconrel.2008.02.013.

Santos, H., Salonen, J., Bimbo, L., Lehto, V., Peltonen, L., Hirvonen, J., 2011. Mesoporous materials as controlled drug delivery formulations.

Sjijberg, S., 1996. Silica in aqueous environments. J. Non Cryst. Solids 196, 51–57.

Song, S.W., Hidajat, K., Kawi, S., 2005. Functionalized SBA-15 materials as carriers for controlled drug delivery: Influence of surface properties on matrix-drug interactions. Langmuir 21, 9568–9575. https://doi.org/10.1021/la051167e.

Suib, S.L., 2017. A Review of recent developments of mesoporous materials. Chem. Rec. https://doi.org/10.1002/tcr.201700025.

Vallet-Regí, M., Balas, F., Arcos, D., 2007. Mesoporous materials for drug delivery. Angewandte Chemie - International Edition. https://doi.org/10.1002/anie.200604488.

Vallet-Regí, M., Colilla, M., Izquierdo-Barba, I., Manzano, M., 2018. Mesoporous silica nanoparticles for drug delivery: current insights. Molecules. https://doi.org/10.3390/molecules23010047.

Vansant, E.F., Van Der Voort, R., Vrancken, K.C., 1995. Studies in Surface Science and Catalysis - CHARACTERIZATION AND CHEMICAL MODIFICATION OF THE SILICA SURFACE. Wilrijk.

Vitha, M., Carr, P.W., 2006. The chemical interpretation and practice of linear solvation energy relationships in chromatography. J. Chromatogr. A. https://doi.org/10.1016/j.chroma.2006.06.074.

Vraníková, B., Niederquell, A., Šklubalová, Z., Kuentz, M., 2020. Relevance of the theoretical critical pore radius in mesoporous silica for fast crystallizing drugs. Int. J. Pharm. 591. https://doi.org/10.1016/j.ijpharm.2020.120019.

Whaley, W.L., Okoso-Amaa, E.M., Womack, C.L., Vladimirova, A., Rogers, L.B., Risher, M.J., Abraham, M.H., 2013. Summation Solute Hydrogen Bonding Acidity Values for Hydroxyl Substituted Flavones Determined by NMR Spectroscopy. Nat. Prod. Commun. 8, 85–98.

Yani, Y., Chow, P.S., Tan, R.B.H., 2016. Pore size effect on the stabilization of amorphous drug in a mesoporous material: Insights from molecular simulation. Microporous Mesoporous Mater. 221, 117–122. https://doi.org/10.1016/j.micromeso.2015.09.029.